

# Linear in-plane magnetoconductance and spin susceptibility of a 2D electron gas on a vicinal silicon surface

Y.Y. Proskuryakov<sup>1,\*</sup>, Z.D. Kvon<sup>2</sup>, A.K. Savchenko<sup>1</sup>

<sup>1</sup> *School of Physics, University of Exeter, Stocker Road, Exeter, EX4 4QL, U.K.*

<sup>2</sup> *Institute of Semiconductor Physics, Novosibirsk, 630090, Russia*

In this work we have studied the parallel magnetoresistance of a 2DEG near a vicinal silicon surface. An unusual, linear magnetoconductance is observed in the fields up to  $B = 15$  T, which we explain by the effect of spin polarization on impurity scattering. This linear magnetoresistance shows strong anomalies near the boundaries of the minigap in the electron spectrum of the vicinal system.

Over the last few years a number of reports have appeared on observations of anomalous positive magnetoresistance (negative magnetoconductance, MC) in high-mobility 2D electron and hole gases in the field parallel to the 2D plane<sup>1</sup>. Such interest is fuelled by the fact that this negative MC is directly related to other unusual properties of high-mobility systems, such as ‘metallic’ behaviour and the transition from ‘metal’ to ‘insulator’<sup>1</sup>. However, until now all studies of in-plane MC were devoted to the range of low electron densities,  $N_s$ , near the ‘metal-insulator’ transition. In the case of a 2D electron gas (2DEG) in Si-MOSFET structures the densities studied were below  $10^{12}$  cm<sup>-2</sup>.

The focus of our study is the in-plane MC in a *vicinal* Si-MOSFET at *high electron densities*,  $N_s > 10^{12}$  cm<sup>-2</sup>. It is well known<sup>2,3,4,5</sup> that this system has a superlattice potential on the Si surface, which results in a minigap in the energy spectrum. Previously, the study of the slow electron diffraction by atomically pure vicinal Si surfaces cut at small angles  $\theta$  to (100) plane (as shown in Fig. 1a) revealed ordered steps, which do not disappear even when specimens are heated up to 1100°C, even in the presence of hydrogen or oxygen<sup>6</sup>. The size of these steps was in agreement with theoretical predictions for perfect high-index surfaces<sup>4</sup>. This periodic structure is considered to be the reason for the appearance of the superlattice potential<sup>3,4</sup>.

The minigap in the energy spectrum has an inter-valley character<sup>4</sup>, which implies a strong inter-valley interaction when the electron energy approaches the minigap. This also leads to the appearance of a logarithmic divergence in the density of states  $D(E)$  at energies close to the lower edge of the minigap, Fig. 1(b).  $D(E)$  differs from zero within the minigap because the superlattice is one-dimensional and does not produce a full gap in the spectrum. The discontinuity in  $D(E)$  also appears at the upper edge of the minigap. When the smearing  $\Gamma$  is less than the width of the minigap  $\Delta$ , transport coefficients exhibit singularities as the Fermi energy  $E_F$  passes through the boundaries of the minigap<sup>3,4,7</sup>.

Such systems with a minigap are of interest because they can realise two different situations: with an isotropic Fermi surface (FS), and an anisotropic one, dependent on the position of the Fermi level. These two cases correspond to different ranges of electron densities, where the

properties of the 2DEG significantly differ:  $N_s < N'_\Delta$  (isotropic FS) and  $N_s > N'_\Delta$  (anisotropic FS), where  $N'_\Delta = \pi(0.15/L)^2$  is the density corresponding to the onset of the superlattice minigap. (Here  $L = a/(2 \sin(\theta))$  is the superlattice period,  $\theta$  is the angle between the vicinal and (100) silicon surface,  $a = 5.43$  Å is the lattice constant of Si.) The properties of the 2DEG in the first range are identical to those of an ordinary (100) Si-MOSFET, while in the second range the properties of the 2DEG become strongly modified<sup>3,4</sup>.

We experimentally investigate the MC in both ranges of  $N_s$ . A linear magnetoconductance is observed in magnetic field parallel to the plane of the 2DEG, in a surprisingly large range of fields up to 15 T. To our knowledge, this is the first observation of such an effect. We describe the linear decrease of the conductance with  $B_{\parallel}$  in terms of the screening model<sup>8</sup>, where impurity scattering gets changed when the 2DEG is spin-polarised by parallel magnetic field. The performed analysis suggests that the slope of the linear MC in the first range of  $N_s$  (isotropic Fermi surface) is in agreement with theoretical expectation for the scattering dominated by impurity potential. In the second range of  $N_s$  a significant decrease of the magnitude of the MC is observed at the boundaries of the minigap. This can be attributed to either the modification of the transport properties of the electrons near the points of topological transitions of the Fermi surface<sup>7,11</sup>, or suppression of the spin susceptibility.

The studied samples are Hall-bar Si-MOSFETs fabricated on a vicinal Si(17,2,2) surface, tilted from (100) by an angle  $\theta = 9^\circ 40'$  around the direction [011]. The superperiod in this case is  $L = 16.2$  Å, which corresponds to  $N'_\Delta \simeq 2.6 \times 10^{12}$  cm<sup>-2</sup>. As this surface is just slightly different from the (811) surface at  $\theta = 10^\circ$ , one can expect qualitatively the same dispersion relation and other properties as those for Si(n11) described in detail in Ref.4. We study the behaviour of the 2DEG for both orientations of the Hall bar – along and perpendicular to the superlattice axis. In the latter case, shown in Fig. 1(a), the peak mobility of the 2DEG is  $\sim 25000$  cm<sup>2</sup>/Vs. Our measurements have been carried out in magnetic fields up to 15 T at  $T \simeq 50$  mK. The experiments have been performed at large electron densities:  $N_s$  from  $1 \times 10^{12}$  to  $5 \times 10^{12}$  cm<sup>-2</sup>.

In magnetic field parallel to the plane of the 2DEG

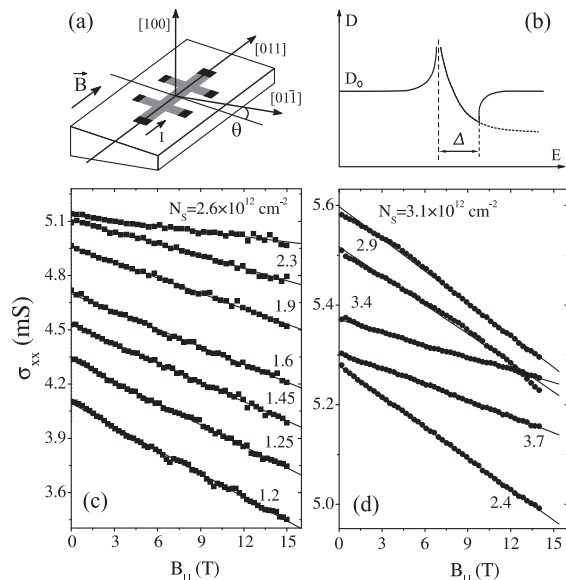


FIG. 1: (a) A schematic diagram showing the geometry of the studied sample in the case of the Hall-bar oriented perpendicular to the super-lattice axis. (b) Density of states of 2DEG in a vicinal sample with super-lattice potential at the surface.  $D_0$  is unperturbed density of states (as in (100)Si MOSFETs), and  $\Delta$  is the minigap width. (c-d) Longitudinal conductivity versus in-plane magnetic field for different electron densities (symbols), with linear fits (solid lines).

we have observed negative MC in the entire range of  $N_s$ . An example is shown in Fig. 1(c, d) for the Hall bar oriented parallel to the superlattice axis. In the whole range of fields the conductivity decreases linearly with  $B_{||}$ . The slope of this linear dependence decreases monotonically with increasing density up to  $N_s \sim 2.5 \times 10^{12} \text{ cm}^{-2}$ , which is close to  $N'_\Delta$ , Fig. 1(c). However, at larger densities the slope starts changing nonmonotonically, as seen in Fig. 1(d). It is important to emphasise that MC remains linear in the entire density range.

In Fig. 2 we show the conductivity measured as a function of electron density at different magnetic fields from 0 to 15 T, for both Hall-bar orientations. In zero magnetic field the so called “ $\Omega$ ”- and “ $W$ ”- features are clearly seen in  $\sigma_{xx}(N_s)$  for the two orientations, respectively (the names reflect the shapes of the two dependences in the minigap). These well known features were previously observed in vicinal systems<sup>3,4</sup>. They originate from the superlattice structure of the vicinal surface and indicate the very good quality of our samples.

One can notice that the effect of magnetic field on the conductivity is minimal in the characteristic points corresponding to the lower and upper boundaries of the superlattice minigap,  $N'_\Delta$  and  $N''_\Delta$ , marked by the vertical dotted lines in Fig. 2 (a,b). This is seen for both Hall-bar orientations and corresponds to the non-monotonic dependence of the linear MC on electron density in Fig. 1(b). Also, a transformation of the “ $W$ ” and “ $\Omega$ ” fea-

tures is seen in Fig. 2 (a,b) – these features seem to be significantly weakened when a strong in-plane magnetic field is applied.

To analyse the linear MC let us first consider the range  $N_s < N_s^\Delta$ , where, as mentioned above, the properties of a 2DEG near the vicinal surface and the (100) surface are expected to be equivalent. Also, it is well established that scattering in the low density regime is dominated by impurity scattering rather than by interface roughness<sup>3</sup>. In this region of  $N_s$  the slope of the linear MC decreases monotonically with increasing density as it has been shown above.

Among several models of negative parallel-field MC<sup>12</sup>, there are two which indeed predict linear MC: one is the interaction theory by Zala, Narozhny and Aleiner<sup>10</sup>, and the other one is the screening model by Dolgoplov and Gold<sup>8</sup>. We start our consideration from the interaction theory, which addresses the effect of in-plane magnetic field on quantum correction to conductivity due to electron-electron ( $e-e$ ) interactions in 2D disordered systems. This theory predicts linear MC in relatively strong magnetic fields and in the ballistic regime, when the parameter  $k_B T \tau / \hbar \gg 1$ . According to Ref. [10] the strong field criterium ( $g^* \mu_B B_{||} / 2k_B T \gg 1$ , where  $g^*$  - Lande g-factor,  $\mu_B$  - the Bohr magneton) is realised in our experiment already at  $B_{||} > 0.3$  T. However the values of the parameter  $k_B T \tau / \hbar$  range from 0.003 to 0.015, implying

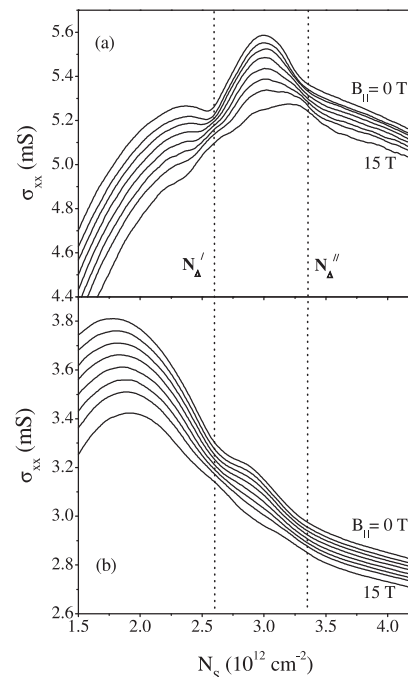


FIG. 2: Density dependence of the conductivity at different in-plane magnetic fields:  $B_{||} = 0, 2, 4, 6, 8, 10, 12, 15$  T; (a) for the Hall-bar oriented perpendicular to the superlattice axis, (b) along the superlattice axis. The dotted lines mark the boundaries of the superlattice minigap at  $N'_\Delta$  and  $N''_\Delta$

that the system is in the diffusive regime,  $k_B T \tau / \hbar \ll 1$ . The estimation of MC caused by electron interactions in this regime<sup>10</sup> shows that effect of  $e-e$  interactions is negligible, as the magnitude of MC (proportional to  $\ln(B)$ ) raises to only about 1% at  $B_{\parallel} \sim 10$  T.

In the screening model<sup>8,9</sup>, developed for the system with isotropic Fermi surface and at  $T = 0$ , the MC effect originates from the change in the screening of scattering potential caused by the difference between Fermi momenta  $k_{F-}$  and  $k_{F+}$  for the two spin-split subbands. It predicts the change of the Drude conductivity with the following negative MC in the low-density case,  $q_s \gg 2k_F$ , where  $q_s$  is the screening wave number. At small magnetic fields  $B_{\parallel}$  such that  $B_{\parallel} < 0.2B_S$ , where  $B_S = 2E_F/g^* \mu_B$  is the field of the full spin polarisation, this MC is linear in the case of short-range impurity scattering:

$$\frac{\sigma(B_{\parallel} < 0.2B_S)}{\sigma(B_{\parallel} = 0)} \simeq 1 - \alpha \frac{B_{\parallel}}{B_S}, \quad (1)$$

where the coefficient  $\alpha$  varies in the range from 0.87 to 0.68 for the electron densities from  $N_s = 1 \times 10^{12}$  to  $5 \times 10^{12} \text{ cm}^{-2}$ , Ref. [8-9]. As the latter is the range of  $N_s$  of our experiment, we take the average value of  $\alpha = 0.78$  for the approximate analysis.

In our case  $q_s/2k_F \sim 2 - 4$  which justifies the approximation of the low density. To justify the applicability of the theory developed for  $T = 0$ , we only analyse quantitatively the data at the lowest temperature  $T = 50$  mK. Simple estimation using standard parameters for (100) Si MOSFETs ( $g^* \sim 2.5$ ,  $m^* = 0.19m_e$ ) gives then 10 – 15% magnetoconductivity in magnetic field  $B \sim 15$  T, which is close to what is seen in Fig. 1(a). The screening theory analyses the effect of magnetic field in both cases of impurity and roughness scattering provided  $B_{\parallel} = B_S$ , Ref. [9]. However, the expression for the small field MC has been obtained only for the impurity scattering, Eq. (1).

As a first approximation, we analyse the slope of the linear dependence in the whole range of electron densities using Eq. (1) and neglecting the influence of interface-roughness scattering. It follows from the above definition of  $B_S$  that  $B_S^{-1} \propto g^* m^*$  and hence it is proportional to the spin susceptibility of the electron gas  $\chi$ . (Indeed, for a 2DEG in a Si MOSFET  $E_F = \pi \hbar^2 N_s / 2m^*$  and  $\chi = 2\mu_B^2 g^* m^* / \pi \hbar^2$ ). The electron density is known from the measurements of Shubnikov–de Haas (SdH) oscillations. From the slope of the linear MC the product  $g^* m^*$  is then found and normalised by  $g_0 m_b$ , where  $m_b = 0.19m_e$  is bulk electron mass ( $m_e$  is the free electron mass) and  $g_0 = 2.0$  is the Lande g-factor in bulk silicon. The data for the both Hall-bar orientations are plotted in Fig. 3(a, b). In Fig. 3(a) we also show the  $g^* m^*$  results obtained by three different experimental groups using the analysis of SdH oscillations in ordinary (100)Si MOSFETs<sup>13,14,15</sup>. At lower densities our results show a monotonic increase of spin susceptibility with decreasing  $N_s$ . This trend at  $N_s \leq 2.3 \times 10^{12} \text{ cm}^{-2}$  as well as the magnitude of  $g^* m^*$  agree well with the previous results. The above range is

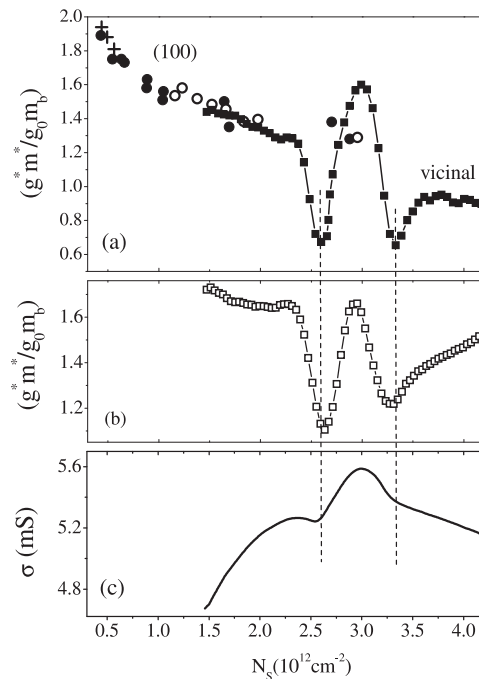


FIG. 3: (a, b) Density dependence of the product  $g^* m^*$  (proportional to spin susceptibility  $\chi$ ) normalised by the product of the bulk parameters  $g_0 m_b$ : (a) for the Hall bar oriented perpendicularly to the superlattice axis, (b) along this axis. Data for (100)Si MOSFETs: (○) - from Ref.[13], (●) - from Ref.[14], (+) - from Ref.[15]. (c) Density dependence of the conductivity at  $B = 0$  for the Hall-bar in case (a) (the same data as in Fig. 2 (a)).

exactly the first range of  $N_s$  we referred to before ( $N_s < N'_\Delta$ ), where the Fermi surface of the vicinal sample is isotropic, as it is in the case of (100)Si, and where the screening theory is valid. This result also indicates that in this range of  $N_s$  the effect of the interface-roughness scattering is negligible.

A strong deviation from the monotonic behaviour of spin susceptibility is observed at larger densities ( $N_s > N'_\Delta$ ) if the analysis is carried out using the same approach as above. A drop of  $g^* m^*$  by more than a factor of two is seen at two different  $N_s$  for the Hall-bar oriented perpendicularly to the superlattice axis, Fig. 3(a). The two minima also appear for the other Hall-bar orientation (along the superlattice axis), Fig. 3(b), although they are less pronounced, presumably because of the smaller mobility of this sample (the difference in the conductivities is seen in Fig. 2). It is clearly seen from the comparison to Fig. 3(c) that these minima coincide with the dips of the “Ω” and “W” features in  $\sigma(N_s)$  – the points where the Fermi level crosses the boundaries of the superlattice minigap. (The pronounced decrease of MC at these points is also seen in Fig. 2 a, b.) It is important to notice that the changes of the conductivity with  $N_s$  at the minigap boundaries do not exceed 10%, Fig. 2, while a much more drastic decrease is seen in the density

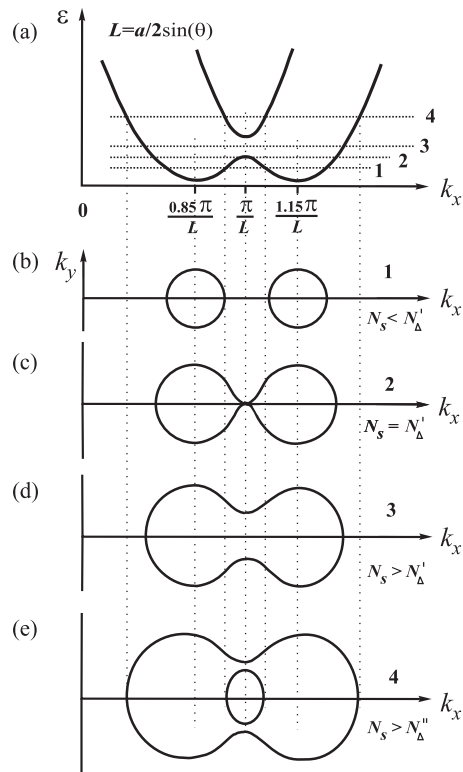


FIG. 4: (a) Typical dispersion relation for a 2DEG in a Si vicinal system<sup>4</sup>. (b-e) Fermi surfaces at different positions of the Fermi level  $E_F$  marked by horizontal dotted lines in (a).

dependence of the spin susceptibility.

We have to note, however, that the screening theory is not expected to be valid in the range of  $N_s > N'_\Delta$ . At the same time, it is seen in Fig. 3(a) that in the middle of the minigap the obtained values of  $g^*m^*$  are close to those obtained for (100)Si using SdH oscillations. This points out that the anomalies in the MC arise only at the boundaries of the minigap.

Let us discuss possible reasons for the dramatic decrease of the MC at the minigap boundaries. A typical dispersion relation of the vicinal system in Si is shown in Fig. 4(a). Different configurations of the Fermi surface

are shown in Fig. 4(b-e) for four positions of the Fermi level. It is seen on the plot that the boundaries of the minigap in the spectrum correspond to the topological transitions of the Fermi surface: firstly the two isotropic and independent FSs coalesce (Fig. 4c), and then they form two inclosed surfaces (Fig. 4e). It is known that the conductivity and thermopower of the electron system is strongly modified at the points of the topological transitions ( $N_s = N'_\Delta, N''_\Delta$ )<sup>4,7</sup>. In our case we see a strong decrease of the linear MC at these points.

The exact theory of MC for complicated FS is not developed. However, if one assumes that the screening theory<sup>8,9</sup> can still be applied at the boundaries of the minigap, our results indicate that the spin susceptibility sharply decreases in the points of the topological transitions. Continuing this logic, it is important to note that previous investigations<sup>11</sup> have shown that the density of states at the minigap boundaries changes only within 10%, which would correspond to a small change in the effective mass. This implies that it is mainly the g-factor that is affected by the topological transitions in the 2DEG spectrum of the vicinal system.

An increase of the g-factor, caused by enhanced exchange interaction, is well known<sup>16</sup>. In contrast, in our case a significant decrease of  $g^*$  (by a factor of two) is observed. This effect could possibly be caused by the strong inter-valley interaction in the vicinal structure (giving rise also to the “Ω” and “W” features in the conductivity<sup>3</sup>). We have to say, however, that the above speculations are based on the assumption that the screening theory<sup>8,9</sup> is applicable within the minigap. An appropriate theory for such a case does not exist at the moment, and we hope that our experiments will stimulate its development.

This work was supported by Royal Society, RFBR (grant 02-02-16516), INTAS (project 01-0014), Russian Ministry of Education (program “Integration”) and RAS (program “Low dimensional quantum structures”), EP-SRC and ORS scheme.

\* Current address: Physics Department, Royal Holloway, University of London, Egham, Surrey, TW20 0EX, U.K.

<sup>1</sup> E. Abrahams *et al.*, Rev. Mod. Phys. **73**, 251 (2001).

<sup>2</sup> L. J. Sham *et al.*, Phys. Rev. Lett. **40**, 472 (1978).

<sup>3</sup> T. Ando, A. Fowler, F. Stern. Rev. Mod. Phys., **54**, 437 (1982).

<sup>4</sup> V. A. Volkov *et al.*, Sov. Phys. Usp. **23**, 375 (1980).

<sup>5</sup> T. G. Matheson and R. J. Higgins, Phys. Rev. B **25**, 2633 (1982).

<sup>6</sup> R. Kaplan, Phys. Semicond. (Inst. Phys. Conf. Ser. Lond.) No. 43, 1351 (1979).

<sup>7</sup> N. V. Zavaritsky, Z. D. Kvon, JETP Lett., **39**, 71, (1984).

<sup>8</sup> V. T. Dolgoplov and A. Gold, JETP Lett. **71**, 27 (2000).

<sup>9</sup> A. Gold and V. T. Dolgoplov, Physica E **17**, 280 (2003).

<sup>10</sup> G. Zala *et al.*, Phys. Rev. B **65**, 020201 (2001).

<sup>11</sup> A. A. Bykov *et al.*, Sov. Phys. Semicond. **22**, 1077 (1988).

<sup>12</sup> B. L. Altshuler *et al.*, Phys. Rev. Lett. **82**, 145 (1999); Y. Meir, Phys. Rev. Lett. **83**, 3506 (1999); S. Das Sarma and E. H. Hwang, Phys. Rev. Lett. **84**, 5596 (2000); I. F. Herbut, Phys. Rev. B **63**, 113102 (2001); V. I. Kozub and N. V. Agrinskaya, Phys. Rev. B **64**, 245103 (2001).

<sup>13</sup> F. F. Fang and P. J. Stiles, Phys. Rev. **174**, 823 (1968).

<sup>14</sup> V. M. Pudalov *et al.*, Phys. Rev. Lett. **88**, 196404 (2002).

<sup>15</sup> T. Okamoto *et al.*, Phys. Rev. Lett. **82**, 3875 (1999).

<sup>16</sup> G.-H. Chen and M. E. Raikh, Phys. Rev. B **60**, 4826 (1999), and references therein.